Electronic Supplementary Material (ESI) for Journal of Materials Chemistry A.

Supplementary Information

Remaking the chlor-alkali electrolysis process to co-generate useful reduction products from CO_2

Yifei Li,[a] Anders Laursen,[a, b] Mahak Dhiman[a] and G. Charles Dismukes *[a, c]

[a]*Department of Chemistry and Chemical Biology, Rutgers, The State University of New Jersey, 610 Taylor Road, Piscataway, New Jersey, 08854*

[b]*418 Orchard Street Cranford, Piscataway, NJ 07016-1745, Renew CO_2*

[c]*Waksman Institute, Rutgers, The State University of New Jersey, 190 Frelinghuysen Road, Piscataway, New Jersey, 08854*

*Corresponding author e-mail: dismukes@rutgers.edu

1. Determination of uncompensated resistance

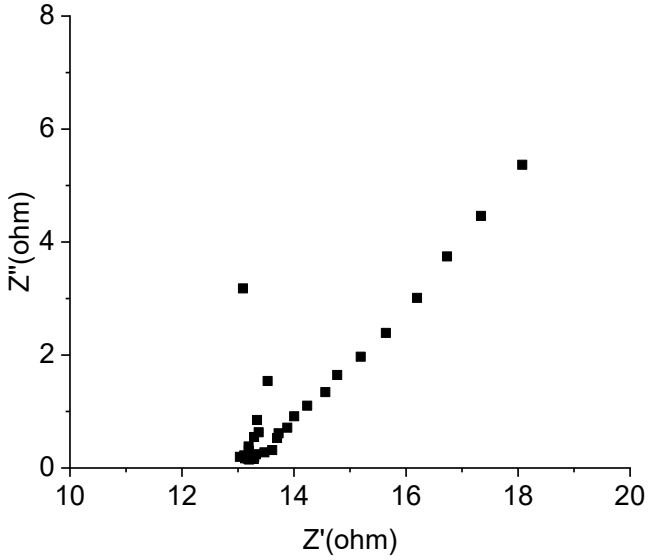

Fig. S1: Potentiostatic electrochemical impedance spectroscopy of the overall cell has resistance of 13 Ω. The electrochemical cell with the cathode, anode, membrane and electrolyte is described in the experimental section.

2. **Linear Sweep Voltammetry**

Linear sweep voltammetry was conducted to compare the performance of Ni_2P in electrolyte comprised of CO_2- saturated 0.5 M $KHCO_3$ (red lines) and in Ar-saturated 0.25 M $Na_4P_2O_7$ (black lines) at the same starting pH, as shown in **Fig. S2**. At more negative potentials, the former gives lower current density, indicating that CO_2 binding to the cathode blocks the HER active sites. However, at applied potentials more positive than -0.2V, the red trace shows higher current density, indicting the relatively higher activity of CO_2RR over HER. This behavior is consistent with thermodynamic control of the product distribution, as we previously reported.

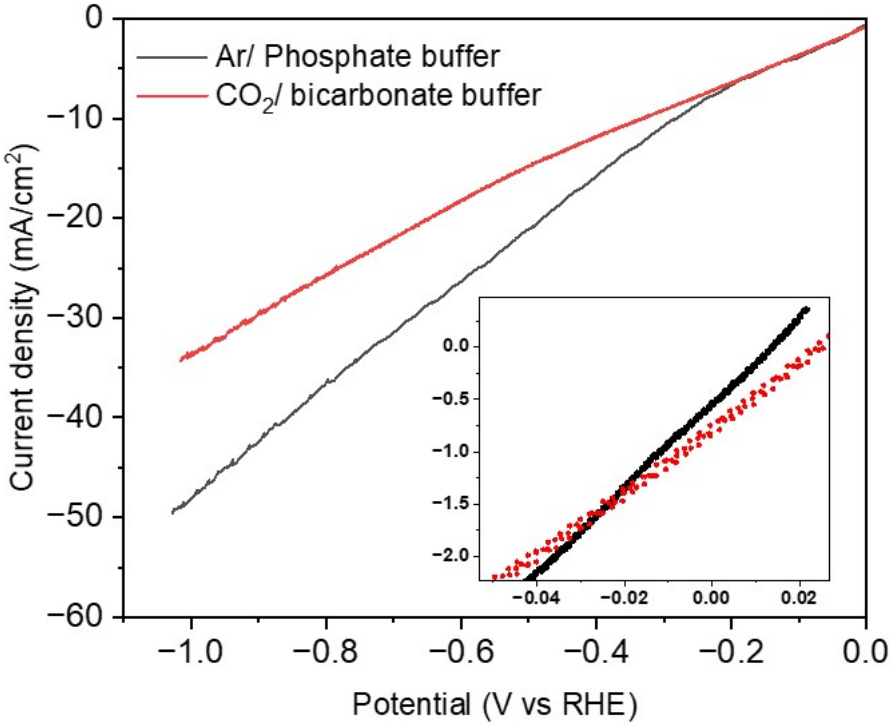

Fig. S2: Linear sweep voltammetry (LSV) for Ni_2P in CO_2-saturated 0 .5 M $KHCO_3$ (red lines) and in Ar-saturated 0.25 M $Na_4P_2O_7$ (black lines) at 10mV/s in cathodic direction.

3. Gas Chromatography

The volatile gas products were analyzed by Gas Chromatograph (GC; SRI model 8610C) with flame ionization detector (FID) and thermal conductivity detector (TCD) in series. Here, the headspace of the cell was directly connected to the GC for online analysis. Volatile gases were separated using a molecular sieve 5A porous layer open tubular capillary column (RT-Msieve 5A) prior to the detectors. The apparatus was purged before reaction to check for air leakage, and then every 1 hour during the measurements.

Samples were taken before reaction to check for air presence and then every hour thereafter. The hydrogen calibration was done with *in situ* generated gas through electrolysis of water on platinum, under argon purge, and diluted post-reaction with CO_2.

The oxygen calibration was done with in situ generated gas through electrolysis of water on platinum.

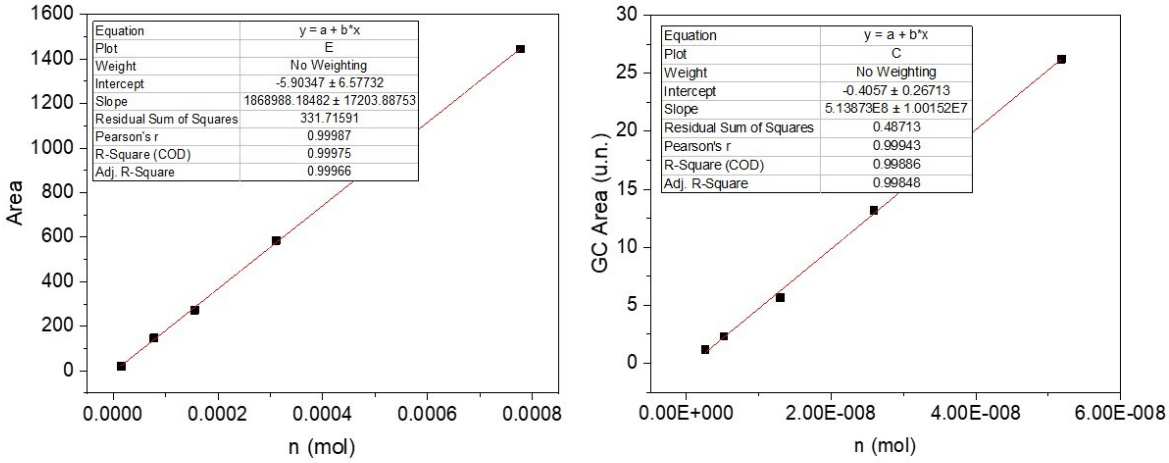

Fig. S3: (a) Calibration curve for hydrogen, the only product detected in the gas phase at the cathode side; (b) Calibration curve for oxygen, the only detected gas product apart from chlorine in the gas phase at the anode side.

4. Liquid Product Analysis by 1H NMR

The 1H NMR sample was made by mixing the 450 µL catholyte taken after the reaction from the working electrode compartment with 150 µL of D_2O. 1H NMR spectra was recorded using a Bruker Avance Neo 500 MHz NMR spectrometer. For the specific details of the assignment of the NMR peaks, please refer to the literature[1].

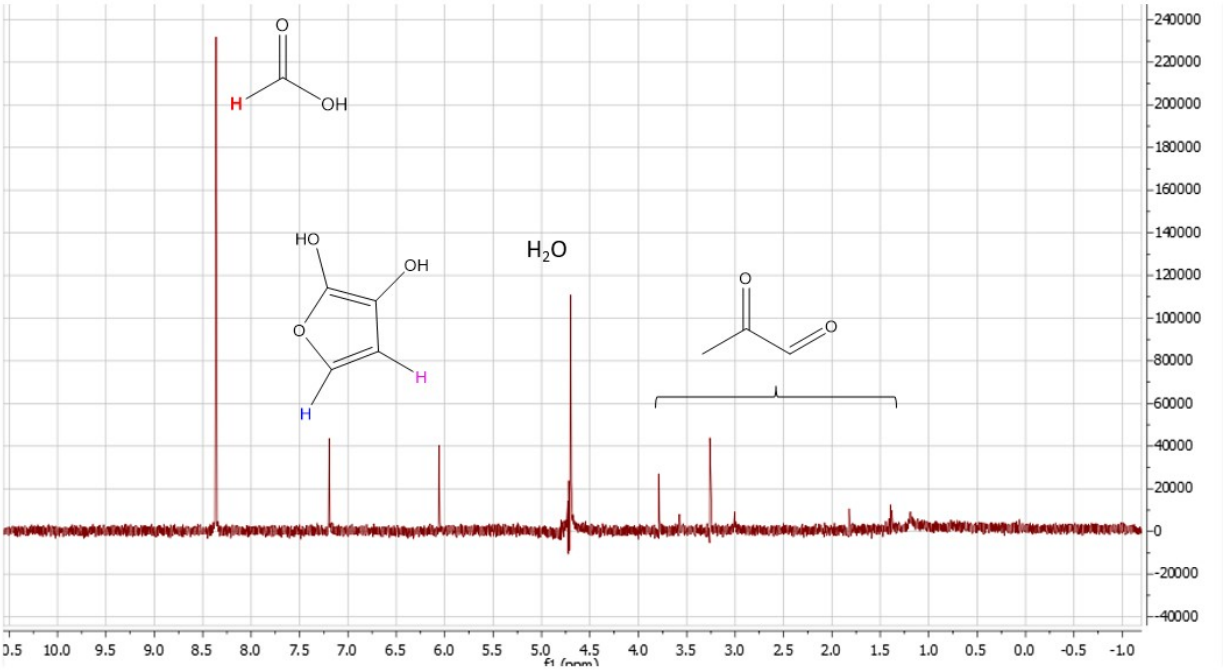

Fig. S4: 1H NMR of a catholyte sample from the electroreduction of CO_2 on Ni_2P(3mA).

5. High Performance Liquid Chromatography

The liquid products were detected and quantified by an offline high-performance liquid chromatography (HPLC; Perkin Elmers Flexer) with an autosampler, UV-vis detector and refractive index detector (RID). Separation was performed on a polymer-based matrix (polystyrene divinylbenzene) column (BioRad HPX 87H Aminex), with injection volumes of 20 µL. The runtime was 60 minutes at a flow rate of 0.3 mL min^{-1} and 45 °C. The calibration ($R^2 > 0.99$) for furandiol, HCOOH and methyl glyoxal was conducted with standards of concentrations ranging from 0.1 to 50 mM. Product assignment was established by retention time and confirmed by 1H NMR (chemical shifts and splitting multiplicity), as described in detail in the ESI and in Calvinho et al.[1]. All measurements were repeated three times on identically prepared and independent samples for statistical significance.

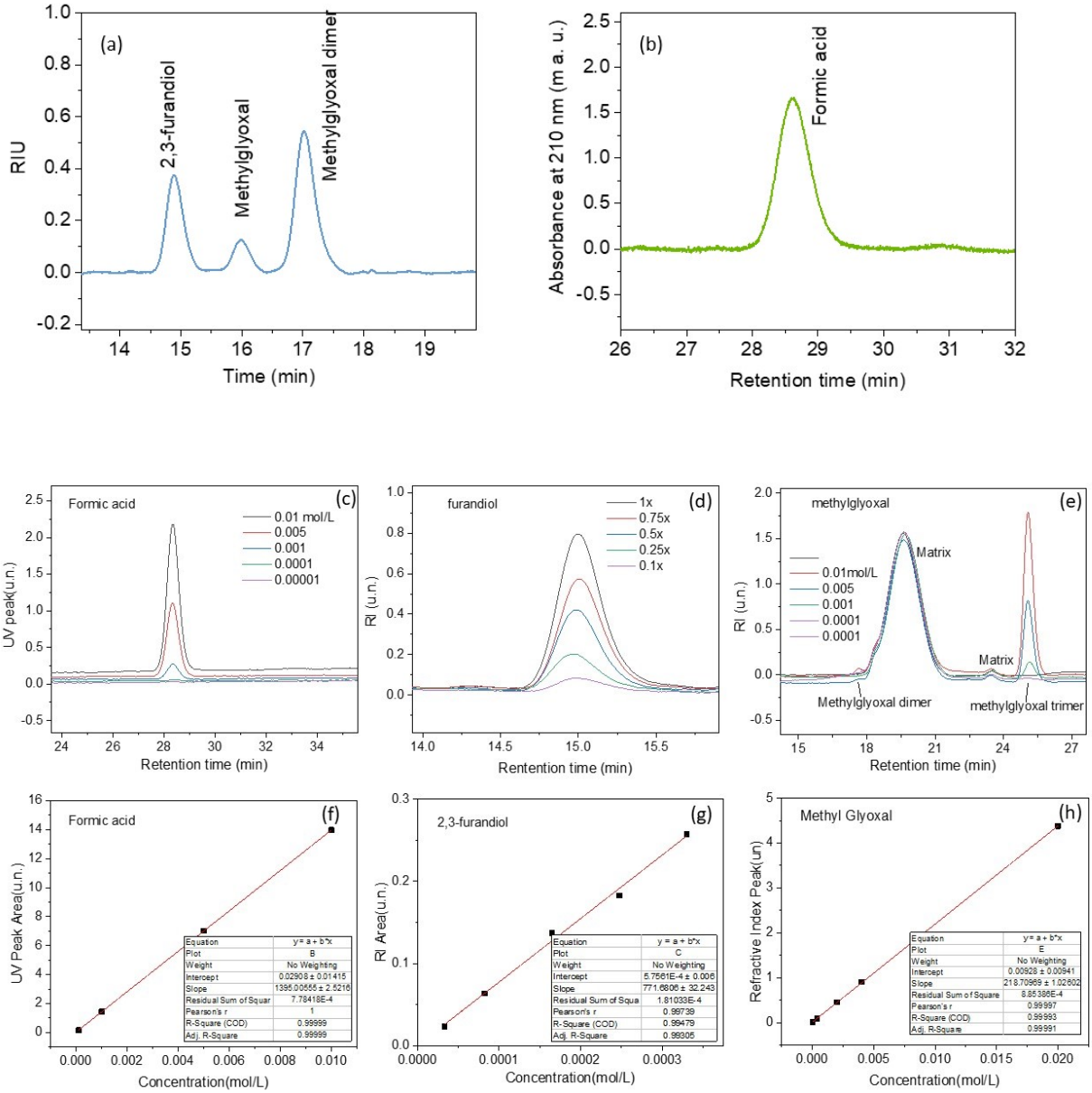

Fig. S5: (a) and (b) Chromatographs for a catholyte sample for CO_2RR on Ni_2P at the current of 1mA obtained with the refractive index detector (left) and the UV absorbance detector (right); (c-h) The HPLC peak for standards of formic acid, 2,3-durandiol and methyl glyoxal and its calibration curves, respectively. The mean error associated with the HPLC quantification was determined to be <1%. The calibration method for methylglyoxal and 2,3-furandiol are the same as the published literature[1].

6. Faradaic Efficiency

The Faradaic Efficiency for the liquid CO_2 reduction products, hydrogen and oxygen was calculated using the equations below, respectively:

$$FECO_2RR = Concentration \cdot Velectrolyte \cdot \#electrons \cdot F/Charge$$

$$FEH_2 = mols\ of\ H_2 \cdot \#electrons \cdot F/\ (current \cdot time)$$

$$FEO_2 = mols\ of\ O_2 \cdot \#electrons \cdot F/\ (current \cdot time)$$

In order to test the remaining charge of oxidation process, a one-time experiment was conducted: argon gas at the flow rate of 20 sccm was purged into the system, went through the 40% NaOH solution and finally connected to the GC to test the oxygen amount, while the chlorine was dissolved in the NaOH solution. At the current of 3 mA, it was calculated that FE(O_2) to be 28%, matches with the FE(Cl_2) of 70%.

Table S1: Faradaic efficiency for all catalysts at the potentials tested ± standard deviation between at least three chronoamperometry experiments.

Current (mA)	Formate Faradic Efficiency (%)	2,3-furandiol Faradic Efficiency (%)	Methylglyoxal Faradic Efficiency (%)	CO_2RR FE (%)	Hydrogen Faradic Efficiency (%)	Total FE (%)
-1	3.15±0.49	20.25±0.77	77.45±0.22	100.85	0	100.85
-2	2.62±0.14	17.36±1.34	74.6±0.52	94.58	5.8±4.1	100.38
-3	3.69±0.1	17.21±0.94	56.67±3.7	77.51	25±7	102.51

7. XRD

The diffraction peaks at 17.4, 26.3, 30.5, 31.7, 35.4, 40.7, 44.6, 47.4, 54.2, 54.9, 57.4, 61.2, 63.5, 66.4, 69.6, 72.7, 74.8, 80.2, 82.9, 86.2, 88.2 and 88.8 are assigned to the (100), (001), (110), (101), (200), (111), (201), (210), (300), (211), (102), (301), (220), (310), (221), (311), (400), (302), (401), (320), (003), (410) and (321) crystal phases, respectively.

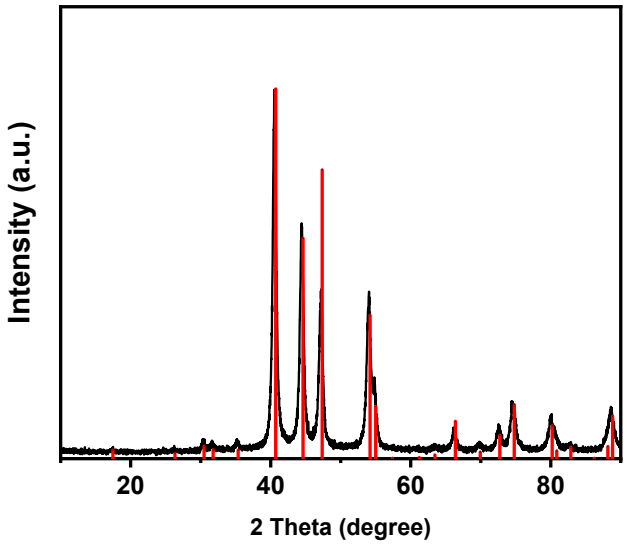

Fig S6. XRD pattern of the Ni_2P synthesized by soft-templated method (black) and reference peak: ICDD # 01-074-1385 (red).

8. XPS

By comparing catalysts without acid washing, we found that Cl still exists as shown in below **Fig. S7a**, and the atomic percentage is 1.34 ± 0.47 %, similar to the Ni_2P catalyst without acid washing (1.49 ± 0.65 %). Therefore, it confirms that the Cl is from the nickel chloride of the synthesis procedure. By further washing the catalyst repeated for 10 times with water, the Cl remains as shown in **Fig. S7b**, indicating the Cl bind with nickel phosphides tightly through chemical binding.

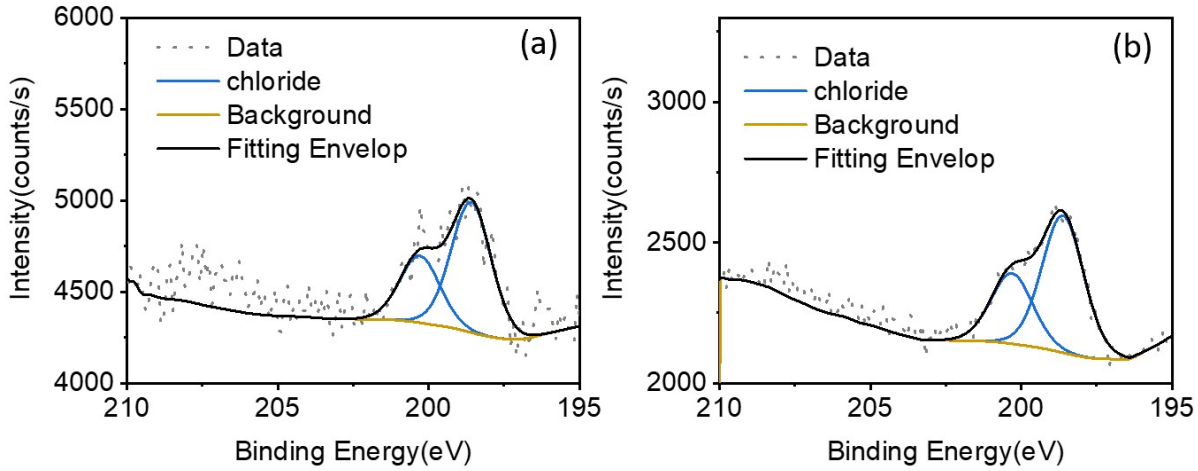

Fig. S7 XPS spectra of Cl 2p of Ni_2P catalyst without acid wash(a); Ni_2P catalyst without acid wash which is further washed with H_2O for 10 times (b).

Table S2. The calculated atomic percentage through XPS analysis was listed for pristine electrodes (sample 1-3); electrodes after catalytic turnover (sample 4-6); pristine electrodes without acid wash (Sample 7-8).

	Pristine electrode (with acid wash)			Electrode after catalytic turnover (with acid wash)			Pristine electrode (without acid wash)	
	Sample 1	Sample 2	Sample 3	Sample 4	Sample 5	Sample 6	Sample 7	Sample 8
Ni	12.42	8.72	10.63	6.94	11.3	14.86	11.22	10.04
O	45.11	42.61	45.67	33.32	41.87	45.82	47.45	45.2
N	1.34	0.7	1.2	8.04	3.96	3.74	1.36	1.15
C	25.54	35.88	28.67	47.01	40.91	32.61	29.8	33.17
Cl	0.63	1.64	2.19	2.84	0.42	0.95	1.8	0.87
P	14.97	10.45	11.64	1.85	1.54	2.01	8.37	9.57

9. Techno-Economic Feasibility

An initial techno-economic feasibility (TEF) model was developed to assess the economic impact of co-generation of methylglyoxal (MG) and chlorine (Cl_2). A TEF model provides a total cost and profit assessment of a plant in the units of $ per day. The costs are categorized into capital costs and operating costs. In this preliminary TEF study we used polarization data obtained at NREL for a single stack MEA type electrolyzer and the same nickel phosphide catalyst supported in a gas diffusion electrode[2]. The capital costs consider only the cost of the electrolyzer and therefore do not include the costs of infrastructure or other downstream or upstream equipment costs. The operating costs include the electricity cost, estimated maintenance cost, and the feedstock costs. The operational lifetime of the plant is assumed to be over 20 years, which is generally considered a conservative estimation for electrochemical processes[3, 4]. The profits are calculated based on the production of all products including MG, Cl_2, $KHCO_3$ and H_2.

We start by calculating the electricity and electrolyzer capital for a plant producing 50,000 kg MG/day. Cell performance upper limit estimate is as follows: cell operating potential of 3.19 V at 50 mA/cm^2 total current density with a 50% FE of MG which will be used as the basis in the following calculations[2]. The cell potential for combined CO_2RR and Cl_2 evolution is estimated starting from the CO_2RR electrolysis using the identical confirmation as follows: 3.06V overall cell potential to operate at 50mA/cm^2 for CO_2RR electrolysis[2], to this is added the additional potential required to produce Cl_2 rather than O_2 at the anode. This added potential is estimated as the standard potential difference between chloride oxidation to Cl_2 (1.36V vs NHE) and water oxidation to O_2 (1.23V)[5]. This calculation implicitly assumes that the overpotential required for chlorine evolution reaction (CER) and oxygen evolution reaction (OER) are similar, together this

gives a cell voltage of 3.19V. Considering CER's faster kinetics (2 electron reaction) compared with OER (4 electron reaction), this is considered a conservative assumption. It should be noted that a far more efficient water electrolysis configuration has recently been demonstrated[6] and this cell type may be applicable to CO_2RR in the future with corresponding decreased operating costs.

As outlined in the main text, the anode current density is actually doubled under the optimized condition to reach up to 100mA/cm^2 due to the smaller anode size. The electrode area used for the electrolyzer capital cost calculations are based on the cathode for simplicity assuming the anode will simply be reduced in size while the rest of the cell structure remains the same.

To estimate the electrolyzer cost we use the basis of the capital costs reported by the hydrogen model (H2A) of the United States Department of Energy for the production of hydrogen via water electrolysis, we make a first level TEF with the cost of the electrolyzer stack is \$423/kW.[7] This model has been widely used in previous CO_2 electroreduction techno-economic analysis[4, 8, 9]. Due to the improvements in water electrolysis costs recent studies estimate the cost of CO_2RR electrolyzers at \$300/kW, making the above a conservative estimate[4]. The parameters used for the TEF calculation are listed in the below Table S3.

Table S3. Parameters for the combined CO_2RR and CER system

Parameter	Value
Overall cell voltage, V	3.19
CO_2 electrolysis current density, mA/cm^2	50
Methylglyoxal faradic efficiency, %	50
Cl_2 faradic efficiency, %	100

Electrolyzer cost, $/kW	423
Electricity cost, ¢/kWh	5.8
Daily methylglyoxal production, kg/day	50,000

(1) **Mass and Energy Flow**

The daily mass of several products (Cl_2, $KHCO_3$, H_2) is calculated by the followed equations:

$$Daily\ product\ mass\left(\frac{kg}{day}\right) = \frac{daily\ methylglyoxal\ production\left(\frac{kg}{day}\right) * product\ molecular\ weight\left(\frac{g}{mol}\right) *}{methylglyoxal\ \ molecular\ weight\left(\frac{g}{mol}\right)}$$

The daily reactant mass (CO_2, H_2O, KCl) consumed is calculated by the equation below:

$$Daily\ reactant\ mass\left(\frac{kg}{day}\right) = \frac{daily\ methylglyoxal\ production\left(\frac{kg}{day}\right) * reactant\ molecular\ weight\left(\frac{g}{mol}\right) *}{methylglyoxal\ \ molecular\ weight\left(\frac{g}{mol}\right)}$$

where the product to methylglyoxal ratio/ reactant to methylglyoxal ratio is obtained from the followed equation (considering the production of methylglyoxal and H_2 at the cathode side, each with 50% faradic efficiency):

$$27CO_2 + 20H_2O + 24KCl \rightarrow C_3H_4O_2 + 12Cl_2 + 24KHCO_3 + 6H_2$$

The KCl usage should be 24 eq of methylglyoxal production due to the according to the equation above (the molecular weight of methylglyoxal is 72g/mol, the molecular weight of KCl is 74.5g/mol):

$$mass\ (KCl) = 50000\frac{kg}{day} \times \frac{mol}{72g} \times 24 \times 74.5\frac{g}{mol} = 1.24 \times 10^6\frac{kg}{day}$$

The CO_2 usage for methylglyoxal:

$$mass\ (CO_2, MG) = \ 50000\frac{kg}{day} \times \frac{mol}{72g} \times 3 \times 44\frac{g}{mol} = 9.17 \times 10^4\frac{kg}{day}$$

The CO_2 usage for $KHCO_3$:

$$mass\ (CO_2, KHCO_3) = \ 50000\frac{kg}{day} \times \frac{mol}{72g} \times 24 \times 44\frac{g}{mol} = 7.33 \times 10^5\frac{kg}{day}$$

The production of H_2:

$$mass\ (H_2) = \ 50000\frac{kg}{day} \times \frac{mol}{72g} \times 6 \times 2\frac{g}{mol} = 8.33 \times 10^3\frac{kg}{day}$$

The usage of H_2O:

$$mass\ (H_2O) = \ 50000\frac{kg}{day} \times \frac{mol}{72g} \times 20 \times 18\frac{g}{mol} = 2.5 \times 10^5\frac{kg}{day}$$

We neglect the charge loss of OER considering the high FE of CER[10], the production rate of Cl_2 should be:

$$mass\ (Cl_2) \ = 50000\frac{kg}{day} \times \frac{mol}{72g} \times 71\frac{g}{mol} \times 12 = 5.92 \times 10^5\frac{kg}{day}$$

The $KHCO_3$ product should be:

$$mass\ (KHCO_3) = \ 50000\frac{kg}{day} \times \frac{mol}{72g} \times 100\frac{g}{mol} \times 24 = 1.67 \times 10^6\frac{kg}{day}$$

The separation cost for $KHCO_3$ could possibly be reduced by utilizing the heat of the *iR* drop from the electrolyzer, however modelling this cost is outside the defined scope of this initial TEF.

(2) Capital cost

The current needed for one day of operation for this 12-electron reduction reaction is:

$$Current(A) = \frac{methylglyoxal\ production(g) * 12e\frac{mol}{molCO2} * 96500C/m}{methylglyoxal\ molecular\ weight\left(\frac{g}{mol}\right) * faradic\ efficiency * 36}$$

$$i = 50000\frac{kg}{day} \times 1000\frac{g}{kg} \times \frac{day}{3600 \times 24s} \times \frac{mol}{72g} \times 12e\frac{mol}{molCO2} \times 965$$

$$10^7\ A$$

The power consumed in a day can be calculated from an estimated operating cell potential of 3.19 V for 50 mA/cm^2 overall current density,

$$Energy\ consumed\ (kW) = Current(A) * Potential_{(V)} * (kW/1000W)$$

$$P = 1.86 \times 10^7 A \times 3.19\ V \times \frac{kW}{1000W} = 5.93 \times 10^4 kW$$

As stated above we choose to use a conservative estimate for electrolyzer costs from B. James et al. developed for water splitting in this first level TEF[11]. The cost of the electrolyzer stack is therefore taken as $423/kW. The electrolyzer is assumed operated at 0.05 A/cm^2 and 3.19V. The installation factor is 1.2 based on the value from B. James et al. Thus, the cost of an electrolyzer capable of producing 50 metric tons/day of MG is:

$$Electrolyzer\ Capital\ cost = Energy\ consumed(kW) * electrolyzer\ cost\left(\frac{\$}{kW}\right) * installation\ factor$$

$$Electrolyzer\ Capital\ cost = 5.93 \times 10^4 kW \times \frac{\$423}{kW} \times 1.2 = 3.01 \times 10^7 \$$$

While water splitting and CO_2RR requires different balance of plant (BoP) technology, the detailed evaluation of this is outside the scope of this initial TEF and the BoP capital cost is considered 10% of the total cost[11], giving a BoP capital cost of

$$BoP = \$1.78 \times 10^7 \times \frac{0.1}{0.9} = \$1.98 \times 10^6$$

Here we used a mature ethanol purification technology to estimate the downstream purification capital cost, which includes purification (distillation, rectifier column, stripping column, molecular sieve, heat exchanger, product tank, and pump) and recycle streams, based on similar mature technology, has a scaled capital cost of \$67226[12].

(3) Operating Costs and Profits

The current electricity cost is calculated from the power requirement and the price of electricity (¢5.8 /kWh based on the average electricity costs in cheap US states like Arkansas, Kentucky, Louisiana, Montana, Oklahoma, Texas, and Washington)[13]:

$$Electricity\ cost\left(\frac{\$}{day}\right) = \frac{Energy\ consumed(kW)}{3600s} * 3600 * \frac{24s}{day} * Electricity\ price\left(\frac{\$}{kWh}\right)$$

$$Electricity\ cost = 5.93 \times 10^4 kW \times \frac{24s}{day} \times \frac{kWh}{3600 \times 1000W} \times \frac{\$0.058}{kWh} = \$8.24 \times 10^4/day$$

The maintenance cost is assumed 3% of capital cost per year based on H2A[7]:

$$\$3.208 \times 10^7 \times \frac{0.025}{year} \times \frac{year}{365day} = \$2{,}636/day$$

The cost of CO_2 is calculated based on a cost of \$130 from[14]:

$$CO_2\ cost = 8.25 \times 10^5 \text{kg/day} \times \frac{\$130}{ton} \times \frac{ton}{1000kg} = \$1.07 \times 10^5/day$$

The cost of H_2O consumption is based on costs of \$1.6/ton from[15]:

$$H_2O\ cost = \ 2.5 \times 10^5 \text{kg/day} \times \frac{\$1.6}{ton} \times \frac{ton}{1000kg} = \$4.0 \times 10^2/day$$

The \$202/ton cost of KCl is based on 2021 numbers due to the abnormal higher costs of KCl in 2023 which are expected to return to normal levels[16]:

$$KCl\ cost = \ 1.24 \times 10^6 \text{kg/day} \times \frac{\$202}{ton} \times \frac{ton}{1000kg} = \$2.50 \times 10^5/day$$

The \$122/ton price of Cl_2 is based on [17] and yields a daily cost of:

$$Cl_2\ cost = 5.92 \times 10^5 \frac{kg}{day} \times \frac{\$122}{ton} \times \frac{ton}{1000kg} = \$7.22 \times \frac{10^4}{day}$$

Using the wholesale price of methylglyoxal as 1.9 \$/kg[18], the daily price of methylglyoxal from this process is:

$$MG\ revenue = \ 5 \times 10^4 \text{kg/day} \times \frac{\$1.9}{kg} = \$9.5 \times 10^4/day$$

The price of H_2 is estimated from[19]:

$$H_2\ revenue = \ 8.33 \times 10^3 \text{kg/day} \times \frac{\$1350}{ton} \times \frac{ton}{1000kg} = \$1.12 \times 10^4/day$$

The \$ 1,089/ton price of $KHCO_3$ is based on [20]:

$$KHCO_3\ cost = \ 1.67 \times 10^6 \text{kg/day} \times \frac{\$1089}{ton} \times \frac{ton}{1000kg} = \$1.82 \times 10^6/day$$

According to the handbook of chlor-alkali technology, the cost of chlorine purification/processing is \$23,400/day when scaled for a 592 ton/day production.[21]

The scaled operating cost for purification technology of methylglyoxal through distillation collumn is $2669/day. [12]

Thus, the net per day profit is:

$$\$ \left(7.22 \times 10^4 + 9.5 \times 10^4 + 1.82 \times 10^6 + 1.12 \times 10^4 - 2.5 \times 10^5 - 1.0\right. \\ /day = \$1.53 \times 10^6/day$$

This initial TEF therefore indicated that the proposed integrated system for co-product generation is competitive in the market at current costs of electricity and feedstocks. Future developments may further improve the commercial impact of this production.

Reference

1. K. U. D. Calvinho, A. B. Laursen, K. M. K. Yap, T. A. Goetjen, S. Hwang, N. Murali, B. Mejia-Sosa, A. Lubarski, K. M. Teeluck, E. S. Hall, E. Garfunkel, M. Greenblatt and G. C. Dismukes, *Energy & Environmental Science*, 2018, **11**, 2550-2559.
2. M. Dhiman, Y. Chen, Y. Li, A. B. Laursen, K. U. D. Calvinho, T. G. Deutsch and G. C. Dismukes, *Journal of Materials Chemistry A*, 2023, DOI: 10.1039/d2ta08173c.
3. J. M. Spurgeon and B. Kumar, *Energy & Environmental Science*, 2018, **11**, 1536-1551.
4. P. De Luna, C. Hahn, D. Higgins, S. A. Jaffer, T. F. Jaramillo and E. H. Sargent, *Science*, 2019, **364**.
5. R. K. Karlsson and A. Cornell, *Chem Rev*, 2016, **116**, 2982-3028.
6. A. Hodges, A. L. Hoang, G. Tsekouras, K. Wagner, C. Y. Lee, G. F. Swiegers and G. G. Wallace, *Nat Commun*, 2022, **13**, 1304.
7. B. James, W. Colella and J. Moton, *PEM Electrolysis H2A Production Case Study Documentation*, 2013.
8. M. Jouny, W. Luc and F. Jiao, *Industrial & Engineering Chemistry Research*, 2018, **57**, 2165-2177.
9. S. Sarp, S. Gonzalez Hernandez, C. Chen and S. W. Sheehan, *Joule*, 2021, **5**, 59-76.
10. H. W. Lim, D. K. Cho, J. H. Park, S. G. Ji, Y. J. Ahn, J. Y. Kim and C. W. Lee, *Acs Catal*, 2021, **11**, 12423-12432.
11. B. James, Colella, Whitney, Moton, Jennie, Saur, G., & Ramsden, T., 2013.
12. Cheng, Wang, Dien, Slininger and Singh, *Processes*, 2019, **7**.
13. Energy Prices Data Explorer, IEA, https://www.iea.org/data-and-statistics/data-tools/energy-prices-data-explorer).
14. https://www.dakotagas.com/Products/pipeline-and-liquefied-gases/liquid-carbon-dioxide.
15. https://waterandsewer.org/commercial/rates/
16. https://ycharts.com/indicators/potassium_chloride_muriate_of_potash_spot_price
17. https://www.chemanalyst.com/Pricing-data/liquid-chlorine-45
18. https://m.chemicalbook.com/ProductDetail_EN_1478932.htm
19. https://www.chemanalyst.com/Pricing-data/hydrogen-1165
20. https://www.echemi.com/productsInformation/pid_Seven12788-potassiumbicarbonate.html
21. T. V. B. Thomas F. O'Brien, Fumio Hine, 2005.